

# Fe<sub>3</sub>O<sub>4</sub>/TiO<sub>2</sub> Core/Shell Nanoparticles as Affinity Probes for the Analysis of Phosphopeptides Using TiO<sub>2</sub> Surface-Assisted Laser Desorption/Ionization Mass Spectrometry

Cheng-Tai Chen and Yu-Chie Chen\*

National Chiao Tung University, Hsinchu 300, Taiwan

Columns packed with microsized titanium dioxide particles have been used effectively as precolumns for enriching phosphopeptides from complex mixtures. Nano-sized titanium dioxide particles have a higher specific surface area and, hence, potentially higher trapping capacities toward phosphopeptides than do microsized particles. Thus, in this study, we employed TiO<sub>2</sub>-coated magnetic (Fe<sub>3</sub>O<sub>4</sub>/TiO<sub>2</sub> core/shell) nanoparticles to selectively concentrate phosphopeptides from protein digest products. Because of their magnetic properties, the Fe<sub>3</sub>O<sub>4</sub>/TiO<sub>2</sub> core/shell nanoparticles that are conjugated to the target peptides can be isolated readily from the sample solutions by employing a magnetic field. In this paper, we also demonstrate that the Fe<sub>3</sub>O<sub>4</sub>/TiO<sub>2</sub> core/shell nanoparticles behave as an effective SALDI matrix: our upper detectable mass limit was ~24 000 Da, whereas the detection limit for peptides was in the low-femtomole range. That is to say, the target analytes trapped by the Fe<sub>3</sub>O<sub>4</sub>/TiO<sub>2</sub> nanoparticles can be identified by introducing the particles directly into the mass spectrometer for TiO<sub>2</sub>-SALDI-MS analysis without the need for any further treatment. For example, elution steps are not necessary when using this approach. In addition, the trapping selectivity of these Fe<sub>3</sub>O<sub>4</sub>/TiO<sub>2</sub> nanoparticles toward phosphopeptides was quite good. These properties combine to result in the low detection limits. The lowest detectable concentration of phosphopeptides that we analyzed using this approach was 500 pM for a 100- $\mu$ L tryptic digest solution of  $\beta$ -casein; this level is much lower than that which can be obtained using any other currently available method.

Phosphorylated proteins play critical roles in regulating biological functions. Generally, the enzymatic digest products of phosphoproteins can be characterized using matrix-assisted laser desorption/ionization mass spectrometry (MALDI-MS), but the signals of the phosphopeptides are often suppressed by the presence of nonphosphorylated peptide residues. Immobilized metal ion affinity chromatography (IMAC) is generally employed to selectively purify phosphorylated peptide residues prior to MS

analysis; the use of immobilized Fe(III) or Ga(III) ions on adsorbents for the purification of phosphopeptides is most common.<sup>1–11</sup>

In addition to Fe(III) and Ga(III), metal oxides may be also applied to selectively concentrate phosphopeptides from complex samples<sup>12–16</sup> because analytes possessing phosphate functional groups can self-assemble onto the surfaces of metal oxide particles;<sup>12–16</sup> monodentate, bidentate, and bidentate-bridging phosphate coordination to metal ions are all possible modes involved in such self-assembly.<sup>17,18</sup> Using this approach, titanium dioxide has been employed for the extraction of phosphates,<sup>19–21</sup> phospholipids,<sup>22,23</sup> and phosphopeptides.<sup>24–26</sup> Previously, we dem-

- (1) Porath, J.; Carlsson, J.; Olsson, I.; Belfrage, G. *Nature* **1975**, *258*, 598–599.
- (2) Posewitz, M. C.; Tempst, P. *Anal. Chem.* **1999**, *71*, 2883–1892.
- (3) Stensballe, A.; Andersen, S.; Jensen, O. N. *Proteomics* **2001**, *1*, 207–222.
- (4) Raska, C. S.; Parker, C. E.; Dominski, A.; Marzluff, W. F.; Glish, G. L.; Pope, R. M.; Borchers, C. H. *Anal. Chem.* **2002**, *74*, 3429–3433.
- (5) Zhang, Y.; Yu, X.; Wang, X.; Shan, W.; Yang, P.; Tang, Y. *Chem. Commun.* **2004**, 2882–2883.
- (6) Zhou, W.; Merrick, B. A.; Khaledi, M. G.; Tomer, K. B. *J. Am. Soc. Mass Spectrom.* **1999**, *11*, 273–282.
- (7) Hart, S. R.; Waterfield, M. D.; Burlingame, A. L.; Cramer, R. *J. Am. Soc. Mass Spectrom.* **2002**, *13*, 1042–1051.
- (8) Thompson, A. J.; Hart, S. R.; Franz, C.; Barnouin, K.; Ridley, A.; Cramer, R. *Anal. Chem.* **2003**, *75*, 3232–3243.
- (9) Stensballe, A.; Jensen, O. N. *Rapid Commun. Mass Spectrom.* **2004**, *18*, 1721–1730.
- (10) Liu, H.; Stupak, J.; Zhang, J.; Keller, B. O.; Brix, B. J.; Fliegel, L.; Li, L. *Anal. Chem.* **2004**, *76*, 4223–4232.
- (11) Hirschberg, D.; Jägerbrink, T.; Samskog, J.; Gustafsson, M.; Ståhlberg, M.; Alvelius, G.; Husman, B.; Carlquist, M.; Jörnvall, H.; Bergman, T. *Anal. Chem.* **2004**, *76*, 5864–5871.
- (12) Folkers, J. P.; Gorman, C. B.; Laibinis, P. E.; Buchholz, S.; Whitesides, G. M. *Langmuir* **1995**, *11*, 813–824.
- (13) Gao, W.; Dickinson, L.; Grozinger, C.; Morin, F. G.; Reven, L. *Langmuir* **1996**, *12*, 6429–6435.
- (14) Brovelli, D.; Hähner, G.; Ruiz, L.; Hofer, R.; Kraus, G.; Waldner, A.; Schüssler, J.; Oroszlan, P.; Ehrat, M.; Spencer, N. D. *Langmuir* **1999**, *15*, 4324–4327.
- (15) Textor, M.; Ruiz, L.; Hofer, R.; Rossi, A.; Feldman, K.; Hähner, G.; Spencer, N. D. *Langmuir* **2000**, *16*, 3257–3271.
- (16) Spencer, N.D.; Textor, R. H. *Langmuir* **2001**, *17*, 4014–4020.
- (17) Kirwan, L. J.; Fawell, P. D.; van Bronswijk, W. *Langmuir* **2003**, *19*, 5802–5807.
- (18) Zhang, Q. L.; Du, L. C.; Weng, Y. X.; Wang, L.; Chen, H. Y.; Li, J. Q. *J. Phys. Chem. B* **2004**, *108*, 15077–15083.
- (19) Kawahara, M.; Nakamura, H.; Nakajima, T. *Anal. Sci.* **1989**, *5*, 763–764.
- (20) Matsuda, H.; Nakamura, H.; Nakajima, T. *Anal. Sci.* **1990**, *6*, 911–912.
- (21) Ikeguchi, Y.; Nakamura, H. *Anal. Sci.* **1997**, *13*, 479–483.
- (22) Ikeguchi, Y.; Nakamura, H. *Anal. Sci.* **1999**, *15*, 229–232.
- (23) Ikeguchi, Y.; Nakamura, H. *Anal. Sci.* **2000**, *16*, 541–543.

\* Corresponding author. Phone: 886-3-5131527. Fax: 886-3-5744689. E-mail: yuchie@mail.nctu.edu.tw.

onstrated that nanocrystalline titania sol-gel-deposited films<sup>27,28</sup> are effective inorganic assisting substrates for TiO<sub>2</sub> sol-gel-assisted laser desorption/ionization mass spectrometry. Tanaka et al. were the first to describe the use of inorganic particles as the matrix for laser desorption;<sup>29</sup> this approach was later termed "surface-assisted laser desorption/ionization mass spectrometry" (SALDI-MS).<sup>30-32</sup> In this study, we examined the feasibility of using TiO<sub>2</sub> nanoparticles for the SALDI matrix; in addition, we investigated how effective the TiO<sub>2</sub> nanoparticles are as specific adsorbents toward phosphopeptides. For convenience during isolation, we coated a thin layer of titania onto the surfaces of magnetic nanoparticles (Fe<sub>3</sub>O<sub>4</sub>/TiO<sub>2</sub> core/shell nanoparticles); these particles then can be isolated readily from the sample solutions once the nanoparticles have trapped the target analytes. The isolated Fe<sub>3</sub>O<sub>4</sub>/TiO<sub>2</sub> core/shell nanoparticles are then ready for TiO<sub>2</sub>-SALDI-MS analysis. To examine the feasibility of using this approach, we employed the tryptic digest products of  $\beta$ -casein and protein phosphatase inhibitor 1 as our model samples.

## EXPERIMENTAL SECTION

**Reagents.** Trifluoroacetic acid (TFA) and hydrochloric acid were obtained from Merck (Seelze, Germany). Iron(III) chloride hexahydrate, ammonium hydrogen carbonate, and diammonium hydrogen citrate were obtained from Riedel-de Haën (Seelze, Germany), and iron(II) chloride tetrahydrate was obtained from Aldrich (Milwaukee, WI). Ammonium hydroxide and tetraethyl orthosilicate (TEOS) were purchased from Fluka (Steinheim, Germany), ethanol was from Showa (Tokyo, Japan), and titanium(IV) butoxide was from Acros (Morris Plains, NJ). Histidine, arginine, angiotensin I, insulin, cytochrome *c*,  $\beta$ -casein (from bovine milk), 2,5-dihydroxybenzoic acid, citric acid, and trypsin (from bovine pancreas) were obtained from Sigma (St. Louis, MO). Human protein phosphatase inhibitor 1 (PPI 1) was kindly provided by Dr. H.-B. Huang (National Chung Cheng University, Taiwan).

**Preparation of Magnetic Nanoparticles.** Fe<sub>3</sub>O<sub>4</sub> nanoparticles were prepared by stirring FeCl<sub>2</sub>·4H<sub>2</sub>O (2 g) and FeCl<sub>3</sub>·6H<sub>2</sub>O (5.4 g) in 2 M hydrochloric acid (25 mL) and degassing the solution using a pump. Ammonia solution [25% (v/v), 30 mL] was added into the mixture, which was then stirred vigorously for 30 min. Nitrogen gas was passed continuously through the mixture during the reaction. The magnetic particles were rinsed with deionized water (3 × 30 mL) and then resuspended in deionized water (50 mL). The concentration of the generated nanoparticles was estimated to be ~40 mg/mL. The nanoparticle solution (5 mL, 40 mg/mL) was then flocculated by positioning a magnet (magnetic field, ~5000 G) adjacent to the sample vial; the solution

was then removed by pipet. Ethanol (2 × 5 mL) was added into the vial to rinse the nanoparticles, followed by sonication for 5 min. The nanoparticles were then dispersed in ethanol (80 mL) under sonication for 1 h.

**Preparation of TiO<sub>2</sub>-Coated Magnetic Nanoparticles.** Ammonia (25%, 8.95 mL), water (7.5 mL), and TEOS (0.15 mL) were added sequentially into the generated magnetic nanoparticle solution, maintained at 40 °C in a water bath, and then the mixture was stirred vigorously for 2 h, followed by sonication for 1 h, to coat a thin layer of SiO<sub>2</sub> onto the surfaces of the magnetic nanoparticles. The nanoparticles were rinsed with ethanol (3 × 30 mL), and then they were resuspended in ethanol (30 mL). This suspension was heated under reflux at 60 °C for 12 h to strengthen the Si-O-Fe cross-linking on the surfaces of the nanoparticles. The SiO<sub>2</sub>-coated magnetic nanoparticles were then flocculated by applying a magnet adjacent to the flask to allow convenient removal of the solution. The nanoparticles were resuspended in ethanol (80 mL), followed by sonication for 1 h. Water (0.15 mL) and ethanol (5 mL) were added into this solution, which was then subjected to vortex-mixing for 15 min. Subsequently, the mixture was combined with a solution of titanium butoxide (0.6 mL) and ethanol (10 mL) and then stirred vigorously in a water bath maintained at 45 °C for 4 h, followed by sonication for 1 h. When the reaction was complete, the magnetic particles in the sample solution were aggregated onto the wall of the flask by positioning a magnet adjacent to the edge of the flask. The remaining solution was then readily removed by pipet. The isolated magnetic nanoparticles were washed repeatedly with ethanol (3 × 30 mL) and distilled water (2 × 30 mL) to remove any unreacted impurities. The magnetic particles were resuspended in distilled water (20 mL) and heated in a water bath at 60 °C to strengthen the cross-linking of TiO<sub>2</sub> onto the surfaces of the nanoparticles. After incubation for 12 h, the nanoparticles were aggregated by positioning a magnet at the edge of the sample bottle, and the solution was removed. The nanoparticles were then stored in distilled water (20 mL) until needed.

**Using Fe<sub>3</sub>O<sub>4</sub>/TiO<sub>2</sub> (Core/Shell) Nanoparticles as a SALDI Matrix.** A solution of Fe<sub>3</sub>O<sub>4</sub>/TiO<sub>2</sub> (core/shell) nanoparticles (20 mg/mL) was prepared by sonicating them for 1 h with a citric buffer comprising diammonium hydrogen citrate (200 mM) and citric acid (200 mM; 5:1.1, v/v). Prior to performing SALDI-MS analysis, the particle solution (0.5  $\mu$ L) was mixed with the analyte solution (0.5  $\mu$ L). A portion of this mixture (0.2  $\mu$ L) was then applied to the sample target. After the solvent had evaporated, the sample was ready for TiO<sub>2</sub>-SALDI-MS analysis.

**Analysis of Phosphopeptides.** Solutions of both  $\beta$ -casein and trypsin were prepared in aqueous ammonium bicarbonate (50 mM, pH 8.2).  $\beta$ -Casein (2 mg/mL, 500  $\mu$ L) and trypsin (2 mg/mL, 10  $\mu$ L), at a weight ratio of 50:1, were incubated at 37 °C for 18 h. The digest product was then diluted in a given volume of TFA solution (0.15%) to adjust the solution to a low pH. Similarly, PPI 1 was digested by trypsin using the same procedures as that outlined above. To perform a trapping experiment, an Fe<sub>3</sub>O<sub>4</sub>/TiO<sub>2</sub> nanoparticle/0.15% TFA solution (20 mg/mL, 0.6  $\mu$ L) was added into the digest product solution (49.4  $\mu$ L). To trap the target species, this mixture was sonicated for 20 s to thoroughly suspend the nanoparticles, followed by vortex-mixing for 90 min. Subsequently, the Fe<sub>3</sub>O<sub>4</sub>/TiO<sub>2</sub> nanoparticles were isolated by positioning

(24) Sano, A.; Nakamura, H. *Anal. Sci.* **2004**, *20*, 565–566.

(25) Sano, A.; Nakamura, H. *Anal. Sci.* **2004**, *20*, 861–864.

(26) Pinkse, M. H.; Uitto, P. M.; Hilhorst, M. J.; Ooms, B.; Heck, A. J. R. *Anal. Chem.* **2004**, *76*, 3935–3943.

(27) Chen, C.-T.; Chen, Y.-C. *Anal. Chem.* **2004**, *76*, 1453–1457.

(28) Chen, C.-T.; Chen, Y.-C. *Rapid Commun. Mass Spectrom.* **2004**, *18*, 1956–1964.

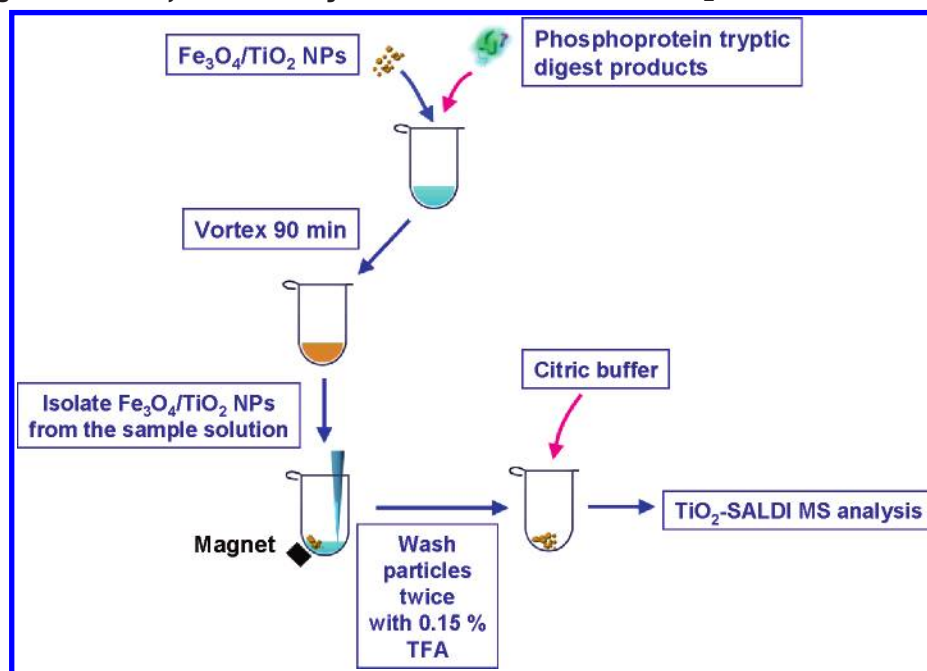
(29) Tanaka, K.; Waki, H.; Ido, Y.; Akita, S.; Yoshida, Y.; Yoshida, T. *Rapid Commun. Mass Spectrom.* **1988**, *2*, 151–153.

(30) Sunner, J.; Dratz, E.; Chen, Y.-C. *Anal. Chem.* **1995**, *67*, 4335–4342.

(31) Dale, M. J.; Knochenmuss, R.; Zenobi, R. *Anal. Chem.* **1996**, *68*, 8, 3321–3329.

(32) Schürenberg, M.; Dreisewerd, K.; Hillenkamp, F. *Anal. Chem.* **1999**, *71*, 221–229.

**Scheme 1. Procedures for the Analysis of Phosphopeptides by Using Fe<sub>3</sub>O<sub>4</sub>/TiO<sub>2</sub> Nanoparticles (NPs) as the Trapping Adsorbents, Followed by the Characterization of TiO<sub>2</sub>-SALDI MS**



a magnet to the outside of the sample vial; the solution was then removed using a pipet. The isolated particles were washed with 0.15%TFA solution ( $2 \times 50 \mu\text{L}$ ) to remove any unbound impurities. Citric buffer solution ( $0.5 \mu\text{L}$ ) was added to resuspend the nanoparticles. The mixture was then applied directly to the sample target. After the solvent had evaporated, the sample was ready for TiO<sub>2</sub>-SALDI-MS analysis. The whole procedure followed for the analysis of the phosphopeptides is displayed in Scheme 1. For comparison, another set of samples was treated in a manner identical to that described above, except that the nanoparticles were replaced by Fe<sub>3</sub>O<sub>4</sub> nanoparticles and Fe<sub>3</sub>O<sub>4</sub>/SiO<sub>2</sub> nanoparticles. The target species trapped by the nanoparticles were identified through MALDI-MS analysis. A mixture of 2,5-dihydroxybenzoic acid (30 mg/mL,  $0.5 \mu\text{L}$ ) and phosphoric acid (1%,  $0.5 \mu\text{L}$ ) was used as the MALDI matrix.

**Instrumentation.** Fourier transform infrared (FTIR) spectra were obtained using a PerkinElmer (Boston, MA) FTIR spectrometer. Scanning electronic microscopy (SEM) images were obtained using a JSM-6500F SEM instrument (JEOL, Japan). All mass spectra were obtained using a Biflex III (Bruker Daltonics, Germany) time-of-flight mass spectrometer equipped with a 337-nm nitrogen laser, a 1.25-m flight tube, and a sample target having the capacity to load 384 samples simultaneously. The linear mode was operated during MS analysis. The accelerating voltage was set at 19 kV, and the laser power was carefully adjusted during analysis to obtain the optimized mass resolution.

## RESULTS AND DISCUSSION

To confirm that we had successfully generated the Fe<sub>3</sub>O<sub>4</sub>/TiO<sub>2</sub> core/shell magnetic nanoparticles, we employed FTIR spectroscopy

to examine the surfaces of the nanoparticles. Figure 1a displays the IR spectrum of the bare magnetic nanoparticles that had not been modified. The characteristic band of Fe<sub>3</sub>O<sub>4</sub> appears<sup>33</sup> at  $\sim 600 \text{ cm}^{-1}$ . After coating a thin SiO<sub>2</sub> layer onto the surfaces of the Fe<sub>3</sub>O<sub>4</sub> nanoparticles, the Si–O–Si stretching vibration bands appears in the FTIR spectrum at  $1091 \text{ cm}^{-1}$ , while the Si–O–H vibration band appears at  $956 \text{ cm}^{-1}$  (Figure 1b).<sup>34,35</sup> The surfaces of the SiO<sub>2</sub>-coated Fe<sub>3</sub>O<sub>4</sub> nanoparticles were then coated with an additional thin layer of TiO<sub>2</sub>. Figure 1c displays the FTIR spectrum of the Fe<sub>3</sub>O<sub>4</sub>/TiO<sub>2</sub> core/shell nanoparticles. We assign the absorption band at  $971 \text{ cm}^{-1}$  to a combination of Si–OH and Ti–O–Si vibrations on the basis of the results of previous studies indicating that the bands of Si–OH groups shift to higher wavenumber (cf. Figure 1b) when Ti–O–Si units are present in a material.<sup>35–37</sup> These FTIR spectroscopy results, therefore, confirm the generation of the Fe<sub>3</sub>O<sub>4</sub>/TiO<sub>2</sub> core/shell nanoparticles.

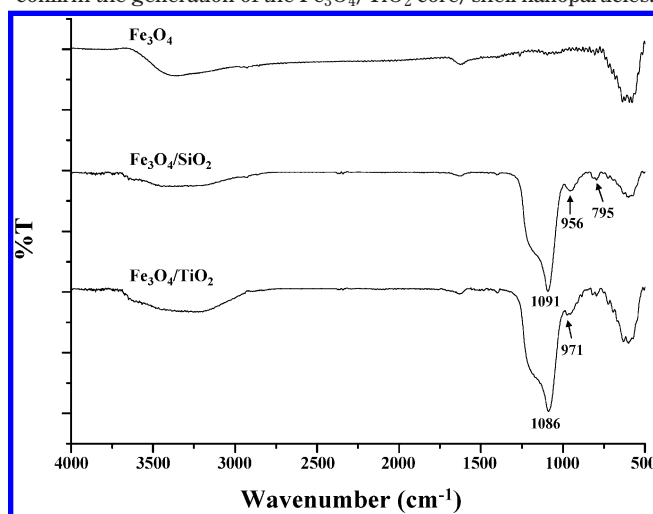
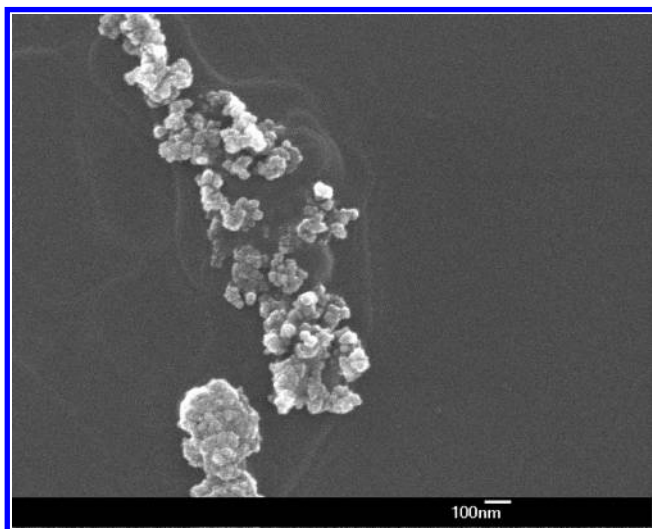


**Figure 1.** FTIR spectra of (a) unmodified bare Fe<sub>3</sub>O<sub>4</sub> nanoparticles, (b) SiO<sub>2</sub>-coated Fe<sub>3</sub>O<sub>4</sub> nanoparticles, and (c) Fe<sub>3</sub>O<sub>4</sub>/TiO<sub>2</sub> core/shell nanoparticles.

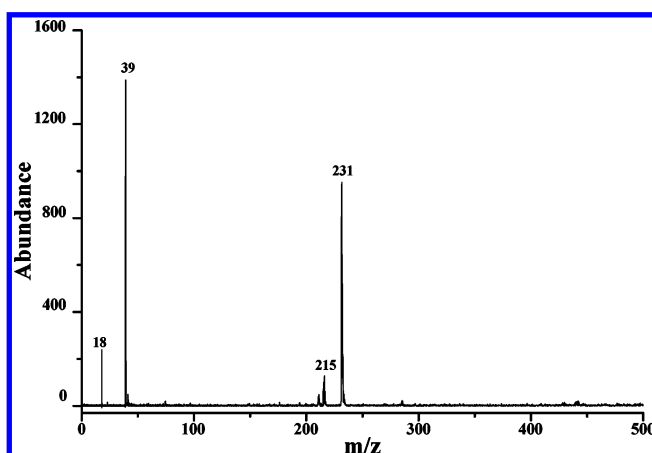
(33) Penk, Z. G.; Hidajat, P. K.; Uddin, M. S. *J. Colloid Interface Sci.* **2004**, *271*, 277–283.

(34) Lü, C.; Cui, Z.; Guan, C.; Guan, J.; Yang, B.; Shen, J. *Macromol. Mater. Eng.* **2003**, *288*, 717–723.

(35) Alba, M. D.; Luan, Z.; Klinowski, J. *J. Phys. Chem.* **1996**, *100*, 2178–2182.



**Figure 2.** SEM image of the  $\text{Fe}_3\text{O}_4/\text{TiO}_2$  nanoparticles.



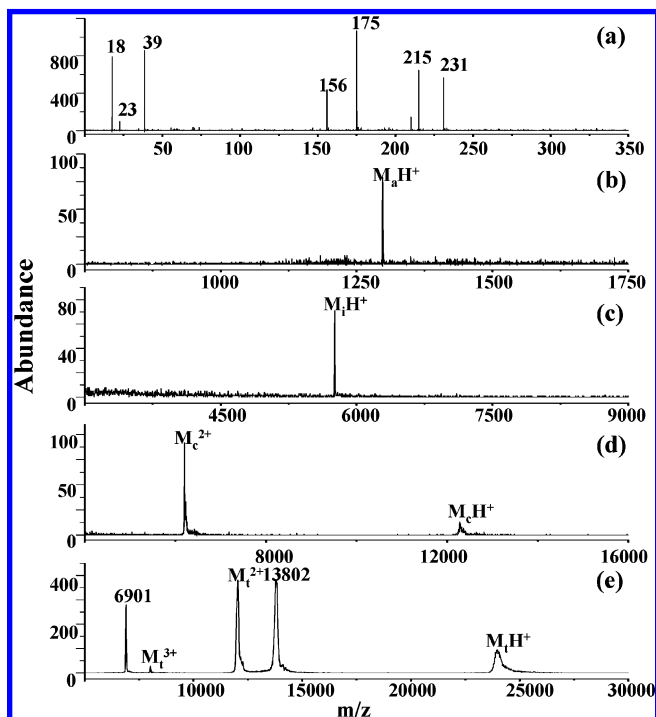
**Figure 3.**  $\text{TiO}_2$ -SALDI mass spectrum of the  $\text{Fe}_3\text{O}_4/\text{TiO}_2$  nanoparticles.

Figure 2 displays an SEM image of the  $\text{Fe}_3\text{O}_4/\text{TiO}_2$  nanoparticles. We estimate the particle size to be  $\sim 50$  nm.

We believed that our magnetic nanoparticles coated with a thin layer of  $\text{TiO}_2$  would behave as a suitable matrix for  $\text{TiO}_2$ -SALDI-MS analysis because, in a previous study, we demonstrated that  $\text{TiO}_2$  sol-gel thin films are suitable matrixes for the analysis of peptides and small proteins using  $\text{TiO}_2$ -SALDI-MS.<sup>28</sup> In addition, we have also demonstrated previously that the addition of a citric buffer to the  $\text{TiO}_2$  sol-gel film can effectively enhance the analyte signals because the citric buffer not only provides an extra proton source for ionization but also can reduce the formation of alkali cation adductions of analytes.<sup>28</sup> Thus, we added a citric buffer to our nanoparticle matrix system. Figure 3 displays the  $\text{TiO}_2$ -SALDI mass spectrum of  $\text{Fe}_3\text{O}_4/\text{TiO}_2$  nanoparticles obtained upon the addition of citric buffer. The potassium ion at  $m/z$  39 dominates the mass spectrum; the peak at  $m/z$  18 corresponds to the  $\text{NH}_4^+$  ion from the ammonium citrate buffer. The peaks at  $m/z$  215 and 231 are the sodium and potassium ion adducts of citric acid.

(36) Kotani, Y.; Matsuda, A.; Kogure, T.; Tatdumisago, M.; Minami, T. *Chem. Mater.* **2001**, *13*, 2144–2149.

(37) Lopez, A.; Tuilier, M. H.; Guth, J. L.; Delmotte, L.; Popa, J. M. *J. Solid State Chem.* **1993**, *102*, 480–191.



**Figure 4.**  $\text{TiO}_2$ -SALDI mass spectra of (a) a mixture of histidine (1.7 pmol) and arginine (300 fmol), (b) angiotensin I (5 fmol), (c) insulin (15 fmol), (d) cytochrome *c* (200 fmol), and (e) trypsinogen (8.5 pmol).

Figure 4a displays the  $\text{TiO}_2$ -SALDI mass spectrum of a mixture of histidine (1.7 pmol) and arginine (300 fmol). The peaks that appear at  $m/z$  156 and 175 correspond to the protonated molecular ions of histidine and arginine, respectively. The peaks appearing at  $m/z$  18, 23, and 39 correspond to the  $\text{NH}_4^+$ ,  $\text{Na}^+$ , and  $\text{K}^+$  ions, respectively. Again, the peaks at  $m/z$  215 and 231 are the sodium and potassium ion adducts, respectively, of citric acid. Figure 4b–e displays the  $\text{TiO}_2$ -SALDI mass spectra of angiotensin I ( $M_a\text{H}^+$ , 5 fmol), insulin ( $M_i\text{H}^+$ , 15 fmol), cytochrome *c* ( $M_c\text{H}^+$ , 200 fmol), and trypsinogen ( $M_t\text{H}^+$ , 8.5 pmol), respectively. The intensities of the multiply charged ions are generally higher than those of the singly charged ions in these spectra. The detection limits for the peptides were in the low-femtomole regime, whereas the upper detectable mass limit was  $\sim 24\,000$  Da when using the  $\text{Fe}_3\text{O}_4/\text{TiO}_2$  nanoparticles as the SALDI matrix. The performance of the  $\text{Fe}_3\text{O}_4/\text{TiO}_2$  nanoparticles used as the SALDI matrix is similar to that of the  $\text{TiO}_2$  sol-gel film.<sup>28</sup>

After demonstrating the capacity of these  $\text{Fe}_3\text{O}_4/\text{TiO}_2$  nanoparticles for use as a SALDI matrix, we further applied them as affinity probes toward phosphopeptides.  $\beta$ -Casein is a common phosphoprotein; we used the tryptic digest product of  $\beta$ -casein as a sample to examine the trapping capacity of the  $\text{Fe}_3\text{O}_4/\text{TiO}_2$  nanoparticles toward phosphopeptides. Figure 5a displays the MALDI mass spectrum of the tryptic digest product of  $\beta$ -casein ( $10^{-6}$  M, 0.5  $\mu\text{L}$ ). Although the peaks appear at  $m/z$  1270.86, 1383.87, 1445.82, 2061.89, 2555.85, and 3122.11 in this mass spectrum, only those at  $m/z$  2061.89, 2555.85, and 3122.11 represent phosphopeptide residues derived from  $\beta$ -casein.<sup>9</sup> Table 1 lists the detailed amino acid sequences for each of these phosphopeptides. Figure 5b presents the  $\text{TiO}_2$ -SALDI mass spectrum of the tryptic digest product of  $\beta$ -casein ( $10^{-6}$  M, 0.5  $\mu\text{L}$ ). Only two peaks appear in the mass spectrum:  $m/z$  1270.73

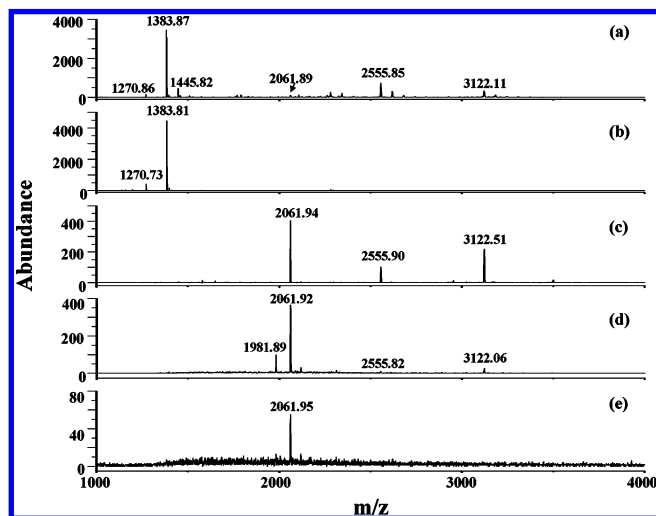


**Figure 5.** (a) MALDI mass spectrum of the tryptic digest product of  $\beta$ -casein ( $10^{-6}$  M,  $0.5 \mu\text{L}$ ). (b)  $\text{TiO}_2$ -SALDI mass spectrum of the tryptic digest product of  $\beta$ -casein ( $10^{-6}$  M,  $0.5 \mu\text{L}$ ). (c–e)  $\text{TiO}_2$ -SALDI mass spectra of the samples obtained when using  $\text{Fe}_3\text{O}_4/\text{TiO}_2$  nanoparticles to selectively trap target peptides from the tryptic digest product of  $\beta$ -casein at the following concentrations and extraction volumes: (c)  $10^{-6}$  M,  $50 \mu\text{L}$ ; (d)  $10^{-8}$  M,  $50 \mu\text{L}$ ; (e)  $5 \times 10^{-10}$  M,  $100 \mu\text{L}$ .

**Table 1. Phosphopeptides Identified in  $\beta$ -Casein<sup>9,38</sup>**

[MH] <sup>+</sup>	peptide residues	phosphopeptide sequence
2061.83	33–48	FQ[pS]EEQQQTEDELQDK
2556.09	33–52	FQ[pS]EEQQQTEDELQDKIHFP
3122.27	1–25	RELEELNVPGEIVE[pS]L[pS][pS][pS]EESITR

and 1383.81. It appears that the signals of the phosphopeptides are totally suppressed in the  $\text{TiO}_2$ -SALDI mass spectrum. Figure 5c displays the  $\text{TiO}_2$ -SALDI mass spectrum of the sample obtained using the  $\text{Fe}_3\text{O}_4/\text{TiO}_2$  nanoparticles to selectively trap target peptides from the tryptic digest product of  $\beta$ -casein ( $10^{-6}$  M,  $50 \mu\text{L}$ ). Only the peaks for phosphopeptide ions ( $m/z$  2061.94, 2555.90, and 3122.51) appear in this mass spectrum. When the concentration of the digest product was decreased by two orders (to  $10^{-8}$  M,  $50 \mu\text{L}$ ), the phosphopeptide peaks at  $m/z$  2061.92, 2555.90, and 3122.51 remained observable in the  $\text{TiO}_2$ -SALDI mass spectrum after we had used the  $\text{Fe}_3\text{O}_4/\text{TiO}_2$  nanoparticles to selectively trap the target peptides (Figure 5d). This result indicates that our nanoparticles can specifically trap and effectively concentrate phosphopeptides from the digest solution. The nanoparticles conjugated to the target peptides can be introduced directly into a mass spectrometer for  $\text{TiO}_2$ -SALDI-MS analysis when citric buffer is added into the samples. The addition of the citric buffer provides an extra proton source and reduces the number of alkali cation adductions of the analytes. Figure 5e displays the  $\text{TiO}_2$ -SALDI mass spectrum of the sample obtained using  $\text{Fe}_3\text{O}_4/\text{TiO}_2$  nanoparticles to selectively trap target peptides from the tryptic digest product of  $\beta$ -casein ( $5 \times 10^{-10}$  M,  $100 \mu\text{L}$ ); this concentration is close to the detection limit ( $50 \text{fmol}$ ) of this approach. This detection limit is  $\sim 2$ – $3$  orders of magnitude lower than those of other current approaches that use IMAC beads combined with MALDI-MS for the analysis of phosphopeptides.<sup>4–6</sup> The lower detection limit may arise from the high trapping

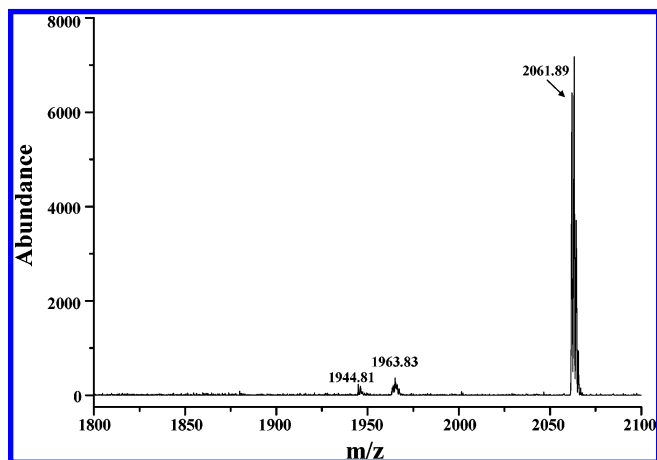


**Figure 6.** PSD  $\text{TiO}_2$ -SALDI mass spectrum of the sample obtained using  $\text{Fe}_3\text{O}_4/\text{TiO}_2$  nanoparticles to selectively trap target peptides from the tryptic digest product of  $\beta$ -casein ( $5 \times 10^{-9}$  M,  $50 \mu\text{L}$ ). The ion at  $m/z$   $2062 \pm 10$  was selected as the precursor ion.

capacity of  $\text{Fe}_3\text{O}_4/\text{TiO}_2$  nanoparticles toward phosphopeptides that occurs because of their extremely small sizes and specificity toward phosphopeptides. Furthermore, the loss of any sample during an elution step is completely avoided when using this direct approach because no such step is required. Figure 6 displays the postsource decay (PSD)  $\text{TiO}_2$ -SALDI mass spectrum of the sample obtained when using  $\text{Fe}_3\text{O}_4/\text{TiO}_2$  nanoparticles to selectively trap target peptides from the tryptic digest product of  $\beta$ -casein ( $5 \times 10^{-9}$  M,  $50 \mu\text{L}$ ). The ion at  $m/z$   $2062 \pm 10$  was selected as the precursor ion. In addition to the peak at  $m/z$  2061.89 ([MH]<sup>+</sup>), the fragment ion at  $m/z$  1963.83 corresponds to the loss of a phosphoric acid unit ([MH – H<sub>3</sub>PO<sub>4</sub>]<sup>+</sup>), and the peak appearing at  $m/z$  1944.81 is the ion obtained after the subsequent loss of a water molecule. This result confirms that the peak at  $m/z$  2061.89 is that of a phosphopeptide.

We further investigated the capacity of our nanoparticles to be selective toward phosphopeptides by analyzing the tryptic digest products other proteins, including cytochrome *c*. Figure 7a presents the  $\text{TiO}_2$ -SALDI mass spectrum of the sample obtained when using  $\text{Fe}_3\text{O}_4/\text{TiO}_2$  nanoparticles to selectively trap target peptides from the tryptic digest product of cytochrome *c* ( $10^{-6}$  M,  $50 \mu\text{L}$ ). The peaks appearing at  $m/z$  1495.70, 1511.66, 1623.79, and 1639.73 correspond to the peptide residues of cytochrome *c*, whereas the peaks at  $m/z$  2163.23 (no.'s 50–69) and 1365.37 (no.'s 137–149) arise from the autolysis of trypsin. Table 2 displays their detailed peptide sequences. Most of these peptides contain several acidic amino acid residues, including glutamic acid and aspartic acid. These results indicate that, in addition to phosphopeptides, the  $\text{Fe}_3\text{O}_4/\text{TiO}_2$  nanoparticles have some degree of trapping capacity toward other acidic peptide residues. Figure 7b present the  $\text{TiO}_2$ -SALDI mass spectrum of the sample obtained using  $\text{Fe}_3\text{O}_4/\text{TiO}_2$  nanoparticles to selectively trap target peptides from the mixture ( $50 \mu\text{L}$ ) of tryptic digest products of cytochrome *c* ( $10^{-6}$  M) and  $\beta$ -casein ( $5 \times 10^{-8}$  M). The peaks appearing at  $m/z$  2062.35, 2556.31, and 3122.14 are those of the phosphopeptides digested from  $\beta$ -casein, and the peaks at  $m/z$  1365.14, 1495.55, 1623.59, 1633.47, and 1751.85 are those from the digest product of either cytochrome *c* or trypsin. This result indicates that the trace phosphopeptides derived from  $\beta$ -casein can be concentrated effectively by the  $\text{Fe}_3\text{O}_4/\text{TiO}_2$  nanoparticles, even when the amount

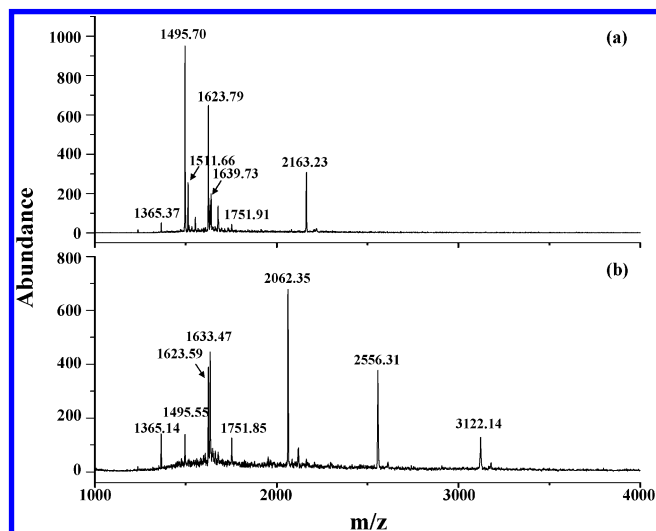


**Figure 7.** TiO<sub>2</sub>-SALDI mass spectra of the samples obtained using Fe<sub>3</sub>O<sub>4</sub>/TiO<sub>2</sub> nanoparticles to selectively trap target peptides from the tryptic digest product of (a) cytochrome *c* (10<sup>-6</sup> M, 50 μL) and (b) a mixture (50 μL) of cytochrome *c* (10<sup>-6</sup> M) and β-casein (5 × 10<sup>-8</sup> M).

**Table 2. Peptides Identified in Cytochrome *c*<sup>a</sup>**

[MH] <sup>+</sup>	peptide residues	peptide sequence
1495.70	61–72	EETLMEYLENPK
1511.69	61–72	EETLMEYLENPK (1 Met-ox)
1623.79	61–73	EETLMEYLENPKK
1633.82	9–22	IFVQKCAQCHTVEK
1639.79	61–73	EETLMEYLENPKK (1 Met-ox)

<sup>a</sup> Searched from <http://tw.expasy.org>

of the tryptic digest product of cytochrome *c* is 20× higher than that of β-casein in the sample solution. As expected, if the concentrations of the tryptic digest solutions of cytochrome *c* and β-casein are almost equal, the phosphopeptide ions generally dominate the TiO<sub>2</sub>-SALDI mass spectra after performing the trapping experiment (results not shown).

We did not observe any phosphopeptide ions generated from β-casein in the TiO<sub>2</sub>-SALDI mass spectrum when we used Fe<sub>3</sub>O<sub>4</sub>/TiO<sub>2</sub> to selectively trap target peptides from a mixture of cytochrome *c* (5 × 10<sup>-6</sup> M) and β-casein (5 × 10<sup>-10</sup> M). Only the ions at *m/z* 1633.51 (no.'s 9–22) and 1495.70 (no.'s 61–72) derived from cytochrome *c* appear in the TiO<sub>2</sub>-SALDI mass spectrum (results not shown). Presumably, the concentration of β-casein is too low to be detected by TiO<sub>2</sub>-SALDI-MS. When we decreased the concentrations of both cytochrome *c* and β-casein to 5 × 10<sup>-10</sup> M, however, the phosphopeptide peaks derived from β-casein appeared at *m/z* 2061.85 and 3122.28 in the TiO<sub>2</sub>-SALDI mass spectrum after using the Fe<sub>3</sub>O<sub>4</sub>/TiO<sub>2</sub> nanoparticles to selectively trap the target peptides from this mixture (see Figure 8a). Because the detection limit of TiO<sub>2</sub>-SALDI-MS is higher than that of MALDI-MS, we obtained enhanced signals for phosphopeptide ions when mixing the Fe<sub>3</sub>O<sub>4</sub>/TiO<sub>2</sub> nanoparticles conjugated with target peptides as the MALDI matrix (see Figure 8b). Three phosphopeptide peaks, at *m/z* 2062.17, 2556.89, and 3122.27, appear in the MALDI mass spectrum.

We also used another phosphoprotein, PPI 1,<sup>39</sup> as a sample to demonstrate the effectiveness of the Fe<sub>3</sub>O<sub>4</sub>/TiO<sub>2</sub> nanoparticles.

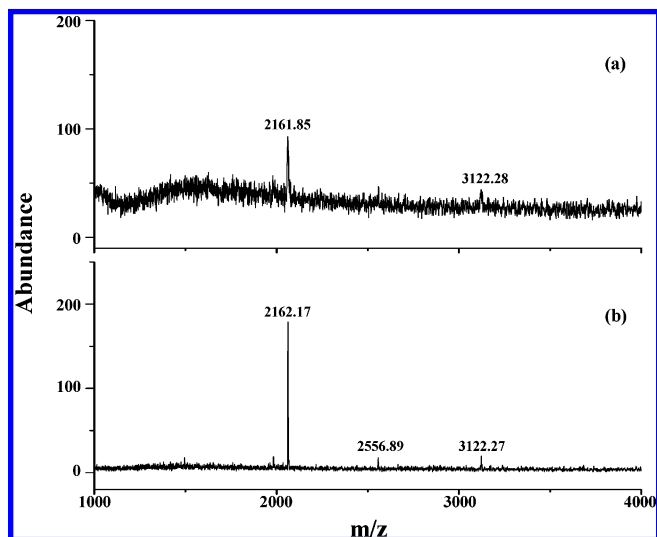


**Figure 8.** (a) TiO<sub>2</sub>-SALDI mass spectrum of the sample obtained using Fe<sub>3</sub>O<sub>4</sub>/TiO<sub>2</sub> nanoparticles to selectively trap target peptides from the tryptic digest product (100 μL) of cytochrome *c* (5 × 10<sup>-10</sup> M) and β-casein (5 × 10<sup>-10</sup> M). (b) MALDI mass spectrum of the Fe<sub>3</sub>O<sub>4</sub>/TiO<sub>2</sub> nanoparticles obtained in part "a" mixed with MALDI matrix. The extraction time was 120 min. A mixture of 2,5-dihydroxybenzoic acid (30 mg/mL, 0.5 μL) and phosphoric acid (1%, 0.5 μL) was used as the MALDI matrix.

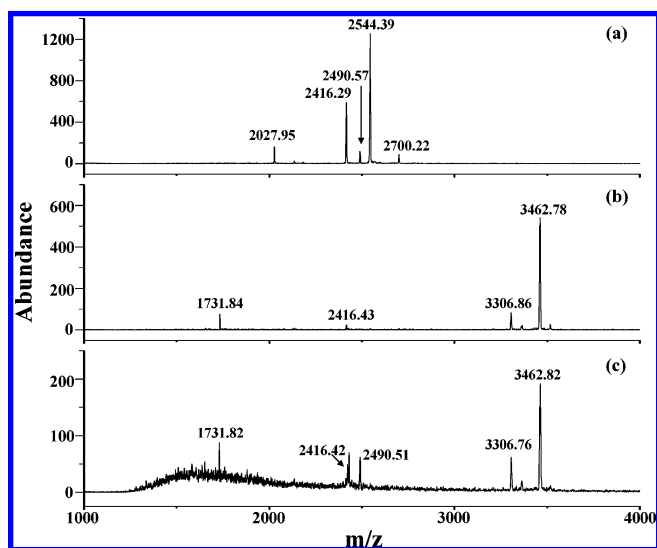


**Figure 9.** (a) TiO<sub>2</sub>-SALDI mass spectrum of the tryptic digest product of PPI 1 (10<sup>-6</sup> M, 0.5 μL). TiO<sub>2</sub>-SALDI mass spectra of the samples obtained when using Fe<sub>3</sub>O<sub>4</sub>/TiO<sub>2</sub> nanoparticles to selectively trap target peptides from the tryptic digest product of PPI 1 at the following concentrations and extraction volumes: (b) 10<sup>-6</sup> M, 50 μL; (c) 5 × 10<sup>-8</sup> M, 50 μL.

Figure 9a displays the TiO<sub>2</sub>-SALDI mass spectrum of the tryptic digest product of PPI 1 (10<sup>-6</sup> M, 0.5 μL). The ion peaks appearing at *m/z* 2027.95, 2416.29, 2544.39, and 2700.22 are nonphosphopeptide residues. Table 3 lists the detailed amino acid sequences for each of these phosphopeptides. Figure 9b displays the TiO<sub>2</sub>-SALDI mass spectrum of the sample obtained using the Fe<sub>3</sub>O<sub>4</sub>/

(38) Deutsch, S.-M.; Molle, D.; Gagnaire, V.; Piot, M.; Atlan, D.; Lortal, S. *Appl. Environ. Microbiol.* **2000**, *66*, 5360–5367.  
 (39) Liu, H.-T.; Lin, T.-H.; Kuo, H.-C.; Chen, Y.-C.; Tsay, H.-J.; Jeng, H.-H.; Tsai, P.-C.; Shie, F.-K.; Chen, J.-H.; Huang, H.-B. *Biochem. Biophys. Res. Commun.* **2002**, *291*, 1293–1296.

**Table 3. Peptide Residues Generated from PPI 1<sup>a</sup>**

[MH] <sup>+</sup>	peptide residues	peptide sequence
2028.08	13–31	TVPILLEPHLDPEAAEQIRR
2416.29	10–30	IQFTVPLLEPHLDPEAAEQIR
2544.38	9–30	KIQFTVPLLEPHLDPEAAEQIR
2700.48	9–31	KIQFTVPLLEPHLDPEAAEQIRR
3306.64	33–61	RP[pT]PATLVLTSDQSSPEIDEDRIPNPHLK
3462.74	32–61	RRP[pT]PATLVLTSDQSSPEIDEDRIPNPHLK

<sup>a</sup> Searched from <http://tw.expasy.org>

TiO<sub>2</sub> nanoparticles to selectively trap target peptides from the tryptic digest product of PPI 1 (10<sup>-6</sup> M, 50 μL). The phosphopeptide peaks appear at *m/z* 3306.86 and 3462.78 (see Table 3). Additionally, a weak peak at *m/z* 2416.43, which is a peptide residue containing several acidic amino acids, appears in this mass spectrum. We were unable to exactly identify the peak at *m/z* 1731.84 from the sequences of the digest product, but we observed that this peak always increased in intensity along with the peak at *m/z* 3462.78. We suspect that this peak might be the doubly charged ion generated from the ion at *m/z* 3462.78, although it is rare to see any doubly charged ions having such a small molecular size (~3500 Da) in traditional MALDI mass spectra. When we decreased the concentration of the digest product 20-fold (5 × 10<sup>-8</sup> M, 50 μL), the phosphopeptide peaks at *m/z* 3306.76 and 3462.82 remained observable in the TiO<sub>2</sub>-SALDI mass spectrum. After we used the Fe<sub>3</sub>O<sub>4</sub>/TiO<sub>2</sub> nanoparticles to selectively trap the target peptides (Figure 9c), we also observed two nonphosphopeptides acidic groups at *m/z* 2416.42 and 2490.51. These results indicate that our nanoparticles can specifically trap and effectively concentrate phosphopeptides from the digest solution, but when the concentration of tryptic digest product is decreased, acidic peptide residues might be observed in the mass spectrum.

The surfaces of conventional IMAC beads generally present immobilized Fe(III); thus, we were interested in determining whether the TiO<sub>2</sub>-coated Fe<sub>3</sub>O<sub>4</sub> nanoparticles have a higher selectivity toward phosphopeptides than do the corresponding bare Fe<sub>3</sub>O<sub>4</sub> particles. Thus, we performed an additional trapping experiment using the bare Fe<sub>3</sub>O<sub>4</sub> particles as the adsorbents and employed MALDI-MS analysis to compare these results with those of the Fe<sub>3</sub>O<sub>4</sub>/TiO<sub>2</sub> nanoparticle-trapped target species. That is, to perform these MALDI-MS analyses, we mixed the MALDI matrix with the nanoparticles after their trapping experiments had been performed. Figure 10a displays the MALDI mass spectrum of the Fe<sub>3</sub>O<sub>4</sub> nanoparticles conjugated to the target peptides after we had used the bare Fe<sub>3</sub>O<sub>4</sub> nanoparticles to trap the target species from the tryptic digest products of β-casein (10<sup>-7</sup> M, 50 μL). We used a mixture of phosphoric acid (1%, 0.5 μL) and 2,5-DHB (30 mg/mL, 0.5 μL) as the MALDI matrix; the addition of phosphoric acid to the MALDI samples can enhance the phosphopeptide ion signals during MALDI-MS analysis.<sup>7</sup> The peak at *m/z* 1396.66 (no.'s 114–125, see Table 4), which is a nonphosphopeptide derived from β-casein, dominates the mass spectrum. The peak at *m/z* 1574.65 (no.'s 126–139, see Table 3), a nonphosphopeptide from β-casein, also appears in the mass spectrum. Both of these peptides (*m/z* 1396.66 and 1574.65) contain acidic amino acids possessing carboxylic acid side chains, such as glutamic acid and aspartic acid. The isoelectric point (pI) of the former ion is 3.79,

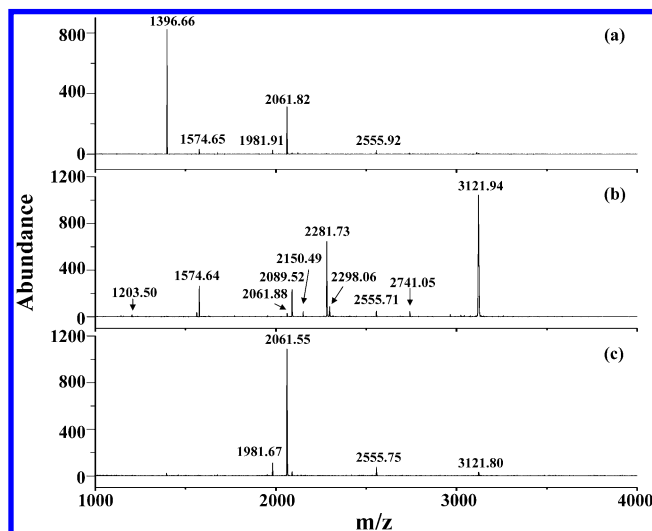


**Figure 10.** MALDI mass spectra of the nanoparticles conjugated to target peptides obtained using (a) Fe<sub>3</sub>O<sub>4</sub>, (b) Fe<sub>3</sub>O<sub>4</sub>/SiO<sub>2</sub>, and (c) Fe<sub>3</sub>O<sub>4</sub>/TiO<sub>2</sub> nanoparticles to selectively trap target peptides from the tryptic digest product of β-casein (10<sup>-7</sup> M, 50 μL). A mixture of 2,5-DHB (30 mg/mL, 0.5 μL) and phosphoric acid (1%, 0.5 μL) was used as the MALDI matrix.

**Table 4. Peptide Residues Generated from β-Casein<sup>a</sup>**

[MH] <sup>+</sup>	peptide residue	peptide sequences
1203.69	134–143	HLPLPLQSW
1396.66	114–125	YPVEPFESQSL
1574.88	126–139	TLTDVENLHPLPL
2089.13	126–143	TLTDVENLHPLPLQSW
2150.12	145–163	HQPHQPLPPTVMFPPQSVL
2281.16	144–163	MHQPHQPLPPTVMFPPQSVL
2741.50	69–93	SLPQNIPLTQTPTVVVPPFLQPEVM

<sup>a</sup> Searched from <http://tw.expasy.org>

whereas that of the latter is 4.35. The presence of acidic amino acids in the peptide residues suggests the reason the Fe<sub>3</sub>O<sub>4</sub> nanoparticles can trap these peptides residues. The peak appearing at *m/z* 2061.82 (no.'s 33–48) is a phosphopeptide derived from β-casein, whereas the peak at *m/z* 1981.91 corresponds to the loss of a phosphoryl group (– PO<sub>3</sub>) from the ion at *m/z* 2061.82. The peak appearing at *m/z* 1981.91 was generally observed in the mass spectrum when the laser power was increased. In addition, another peak, at *m/z* 2555.92 (no.'s 33–52), is that of a phosphopeptide derived from β-casein. These results indicate that the bare Fe<sub>3</sub>O<sub>4</sub> nanoparticles are capable of trapping both acidic peptide residues and phosphopeptides from digest solutions. Figure 10b presents the MALDI mass spectrum of the nanoparticles conjugated to target peptides that we obtained when using Fe<sub>3</sub>O<sub>4</sub>/SiO<sub>2</sub> nanoparticles to selectively trap target peptides from the tryptic digest product of β-casein. The phosphopeptide at *m/z* 3121.94 dominates the mass spectrum; another two phosphopeptides having weak intensities also appear in the mass spectrum at *m/z* 2061.88 and 2555.71. The peptide residues no.'s 126–139, 126–143, and 69–93 (see Table 4) containing several acidic amino acids appear in the mass spectrum. Additionally, the peptide residues no.'s 134–143, 145–163, and 144–163 (see Table 4), which do not contain any acidic amino acids, also appear in this mass spectrum. These results indicate that not only can the Fe<sub>3</sub>O<sub>4</sub>/SiO<sub>2</sub> nanoparticles

bind to the phosphopeptides but also that they are capable of binding to either acidic or nonacidic peptide residues. The Fe<sub>3</sub>O<sub>4</sub>/SiO<sub>2</sub> nanoparticles have no specific selectivity toward phosphopeptides. Figure 10c presents the MALDI mass spectrum of the Fe<sub>3</sub>O<sub>4</sub>/TiO<sub>2</sub> nanoparticles conjugated to target peptides; we obtained this spectrum when using the Fe<sub>3</sub>O<sub>4</sub>/TiO<sub>2</sub> nanoparticles to trap target peptides from the tryptic digest products of  $\beta$ -casein (10<sup>-7</sup> M, 50  $\mu$ L). A solution of phosphoric acid (1%) and 2,5-DHB was mixed with the nanoparticles prior to their MALDI-MS analysis. An intense peak, appearing at  $m/z$  2061.55, dominates the mass spectrum, whereas the peak at  $m/z$  1981.67 corresponds to the ion at  $m/z$  2061.67 having lost a phosphoryl group. The peaks appearing at  $m/z$  2061.55, 2555.75, and 3121.80 represent phosphopeptides derived from  $\beta$ -casein. Although the peptide residues no.'s 114–125, 126–139, 126–143, and 69–93 at  $m/z$  1396.66, 1574.88, 2089.13, and 2741.50 (see Table 4), respectively, have calculated pI values of  $\sim$ 4 and contain several acidic amino acids, they cannot be trapped selectively by the Fe<sub>3</sub>O<sub>4</sub>/TiO<sub>2</sub> nanoparticles. Because no acidic peptide residues were observed in the mass spectrum after trapping treatment, our results indicate that the Fe<sub>3</sub>O<sub>4</sub>/TiO<sub>2</sub> nanoparticles have a very high specificity toward phosphopeptides. Indeed, the selectivity of these Fe<sub>3</sub>O<sub>4</sub>/TiO<sub>2</sub> nanoparticles toward phosphopeptides is much higher than that of the corresponding bare Fe<sub>3</sub>O<sub>4</sub> and Fe<sub>3</sub>O<sub>4</sub>/SiO<sub>2</sub> nanoparticles.

In this approach, we did not elute the peptides after using our nanoparticles to trap the target peptides. The nanoparticles were introduced directly into the mass spectrometer for analysis. Nevertheless, we used absorption spectropic analysis to estimate the recovery efficiency of  $\beta$ -casein adsorbed on the surfaces of Fe<sub>3</sub>O<sub>4</sub>/TiO<sub>2</sub> nanoparticles after being eluted by 1% NH<sub>4</sub>OH. The

recovery efficiency is estimated to be  $\sim$ 51%. The result indicates that using TiO<sub>2</sub>-SALDI-MS directly as the detection method can avoid the problem of sample loss during elution.

## CONCLUSIONS

We have demonstrated that Fe<sub>3</sub>O<sub>4</sub>/TiO<sub>2</sub> core/shell magnetic nanoparticles are an effective SALDI matrix that can be used in TiO<sub>2</sub>-SALDI-MS analyses for the detection of analytes having masses of up to 24 000 Da. Furthermore, we have confirmed that these Fe<sub>3</sub>O<sub>4</sub>/TiO<sub>2</sub> core/shell nanoparticles have quite a good selectivity toward phosphopeptides in mixture solutions. The method for fabricating these nanoparticles is straightforward because there is no need to modify any organic chelating agent onto the surface of the Fe<sub>3</sub>O<sub>4</sub>/TiO<sub>2</sub> magnetic nanoparticles. On the basis of their magnetic properties, nanoparticles that are conjugated with target peptides can be isolated readily from sample solutions. The nanoparticles can be analyzed directly through TiO<sub>2</sub>-SALDI-MS without the need for any elution steps; this feature greatly reduces the analysis time. Taking all of these features together, this approach is a sensitive and effective method for the analysis of phosphopeptides.

## ACKNOWLEDGMENT

We thank the National Science Council (NSC) of Taiwan for supporting this research financially. We also thank Y.-T. Wu for her assistance in preparing the Scheme.

Received for review May 13, 2005. Accepted July 12, 2005.

AC050831T